New insights on physicochemical features and toxicological outcome provided from incineration of nanocomposites

Claire Longuet, Carine Chivas-Joly, Nora Lambeng, Valérie Forest, Lara Leclerc, Gwendoline Sarry, Jérémie Pourchez, J. Lopez-Cuesta

Next Nanotechnology 7 (2025) 100113

Contents lists available at ScienceDirect

Next Nanotechnology

journal homepage: www.sciencedirect.com/journal/next-nanotechnology

Research article

New insights on physicochemical features and toxicological outcome provided from incineration of nanocomposites

Claire Longuet [a,*], Carine Chivas-Joly [b], Nora Lambeng [b], Valérie Forest [c], Lara Leclerc [c], Gwendoline Sarry [c], Jérémie Pourchez [c], José-Marie Lopez-Cuesta [a]

[a] Polymers Composites and Hybrids (PCH), IMT Mines Ales, 6 Avenue de Clavières, Alès 30319, France
[b] LNE – Laboratoire National de Métrologie et d'essais, DMSI, CARMEN Plateform, 29, Avenue Roger Hennequin, Trappes 78197, France
[c] Mines Saint-Etienne, Univ Jean Monnet, INSERM, U 1059 Sainbiose, Centre CIS, Saint-Etienne 42023, France

ARTICLE INFO

Keywords:
Nanocomposites end-of-life
Nanoparticles
Silica
Calcium carbonate
Toxicity
Dimensional characterizations

ABSTRACT

This study focuses on research in the area of "nanomaterials in waste" and shows the difficulty of providing quantitative data on nanomaterials in different wastes. As highlighted in the ECHA report (November 2021) and although substantial progress have been made in the characterization and measurement of nanomaterials, some challenges remain, particularly the characterization of nanomaterials in complex media. Therefore, work to improve the detection, characterization, and quantification of nanomaterials should be continued to complete the database with different types of nanowaste mixtures. The dominant end-of-life scenario for nanocomposites is the incineration. The environmental by-products impact on the soil and air have been considered from the point of view of nanoparticles partitioning and the potential toxicological synergistic effects. A specific management of nanocomposites end-of-life should be implemented as recommended by the Organization for Economic Co-operation and Development (OECD) in order to limit nanoparticles dissemination by landfilling and particularly in incineration facilities where their presence is significantly increasing. The aim of our study was to expand the current knowledge of the partition of nanowaste, mainly in case of nanocomposites mixture, and the potential synergetic or antagonistic impact of potential hazardous nanowastes on the toxicological profile. Incineration products of ethylene-vinyl acetate copolymer (EVA) and polydimethylsiloxane (PDMS) nanocomposites containing both silica and precipitated calcium carbonate, corresponding to cable sheaths compositions, were investigated in this study, using a lab-scale incineration process. Soot and residue composition were analysed using various relevant experimental techniques in order to assess the presence of initial nanoparticles. *In vitro* toxicological assessments were carried out and have shown that only pro-inflammatory responses seem to be affected by the presence of nanoparticles. SiO_2 nanoparticles appear to have a major impact on toxicity whatever the partitioning in soot or residue. Conversely, $CaCO_3$ as expected does not impact the nanowaste toxicity and does not seem able to mitigate the SiO_2 toxicity.

1. Introduction

Many industrial sectors and applications (cosmetic, building, automobiles, aeronautic, aerospace industry, etc.) benefit from the extraordinary nanocomposites properties [1]. In 2022, the worldwide plastics production was estimated to 400.3 million metric tons, and, in Europe to 58.7 million metrics tons [2]. In the European building industry, the electrical and electronic sector accounts for 6.2 % (3.17 million tons) of the total plastics processors demands [3]. From the end of the nineties, the wire and cable industry has been one of the main consumers of nanoparticles to create nanocomposites endowed with flame retardant properties among others [4,5].

Despite their considerable interest, nanocomposites may have adverse environmental impacts, from the different phases of their life-cycle to their end-of-life [6-8]. In particular, one of the main issues regarding incineration is the potential biological effects that may be induced by the incineration by-products of nanocomposites that may contain nanoparticles. The knowledge about the fate of nanoparticles during incineration of nanocomposites is still limited [9,10]. From the few existing studies the fate of nanoparticles in wastes cannot be

* Correspondence to: IMT Mines Alès, 6 avenue de Clavières, Alès 30319, France.
E-mail address: claire.longuet@mines-ales.fr (C. Longuet).

https://doi.org/10.1016/j.nxnano.2024.100113
Received 30 May 2024; Received in revised form 1 October 2024; Accepted 8 October 2024
Available online 21 October 2024

generalized [11-17,7].

A specific management of the end-of-life of nanocomposites should be implemented as recommended by the Organization for Economic Co-operation and Development (OECD) [10,18] in order to avoid nanoparticles dissemination by landfilling and particularly in incineration facilities where their presence is significantly increasing [15,19]. Despite the increasing efficiency of gas treatments, the potential hazard profile of nanoparticles can be exacerbated during incineration processes, owing to surface chemistry modifications, aggregation or adsorption phenomena [20]. In some cases, it was demonstrated that high temperatures can lead to partial or total fragmentation, oxidation or combustion of organic nanoparticles, even if inorganic ones can be aggregated with soot. Various incineration conditions can be found using temperatures between 850 and 1100°C [7]. To address the lack of data, lab-scale experimental platforms have been developed to investigate and reproduce the end-of-life scenario in link with standard industrial incineration conditions such as the temperature, the oxygen concentration, the residence time and the fuel turbulence [21–23,7,20].

After incineration, two kinds of residues can have emerged. The question of the state and the fate of NPs and their potential toxicity of this residual part (*i.e.* nanoparticles present in residues or soot after incineration) have not been widely studied. Yet, toxicological studies using *in vitro* assays are important to assess the hazard associated to the release of ultrafine particles from the incineration of nanocomposites [12,16,24]. Indeed, although some laboratory studies on different types of nanocomposites have highlighted the presence of nanoparticles in residues or soot, they have not addressed the impact on risk resulting from a mixture of nanoparticles that may be present in the waste stream.

The experimental investigations on the partitioning of nanowaste after incineration process is essential to perform toxicological profile and to reproduce real-life scenarios of exposure for predicting the environmental concentrations of nanoparticles in model calculations.

The main objectives of this study are to improve the current comprehension of the partition of nanowaste and the potential synergetic or antagonist impact of potential hazardous nanowastes on toxicological profile.

Our specific aims were as follows:

(i) to examine the fate of a mixture of nanoparticles (SiO_2 and $CaCO_3$) incorporated in EVA or PDMS polymer matrix in order to determine their release and by-products distribution in soot or residue ash;
(ii) to elucidate transformation or destruction of nanostructures during the combustion process and the possible unchanged release of nanoparticles;
(iii) to explore potentially nanoparticles synergistic effect on biological outcomes.

The presence of a mixture of nanoparticles in nanocomposite incinerated with polymer blends of polyamide 6 and polypropylene (PA-6/PP) containing ZnO nanoparticles [25] leads to biological activities related to ZnO nanowaste in these residues. To better understand the interactive effects and mechanisms between the mixture of NPs (ZnO, SiO_2 and $CaCO_3$), we focused our study on polyolefin polymer blends (PA-6/PP) associated with EVA, which are widely present in waste streams and which generate no residues.

Hence, chemical, physical, and morphological changes of by-products from nanocomposites and mix nanoparticles, and the *in vitro* hazards arising from the mixture of these by-products have been investigated. For this purpose, a macrophage cell line was used to assess cytotoxicity in terms of induction of cell death (LDH (Lactate DeHydrogenase) release assay), pro-inflammatory response (TNF-α (Tumor Necrosis Factor) production) and oxidative stress (production of ROS (reactive oxygen species)).

2. Materials and methods

The combination of existing set-up (Lab-Scale incinerator developed in 2015 by Ounoughene et al.) and the experimental mixture of wastes streams are necessary to fully characterize nanowaste and feed further toxicological models.

2.1. Materials

The ethylene-vinyl acetate copolymer (EVA) used was PA440 from Repsol and polydimethylsiloxane (PDMS, High Temperature

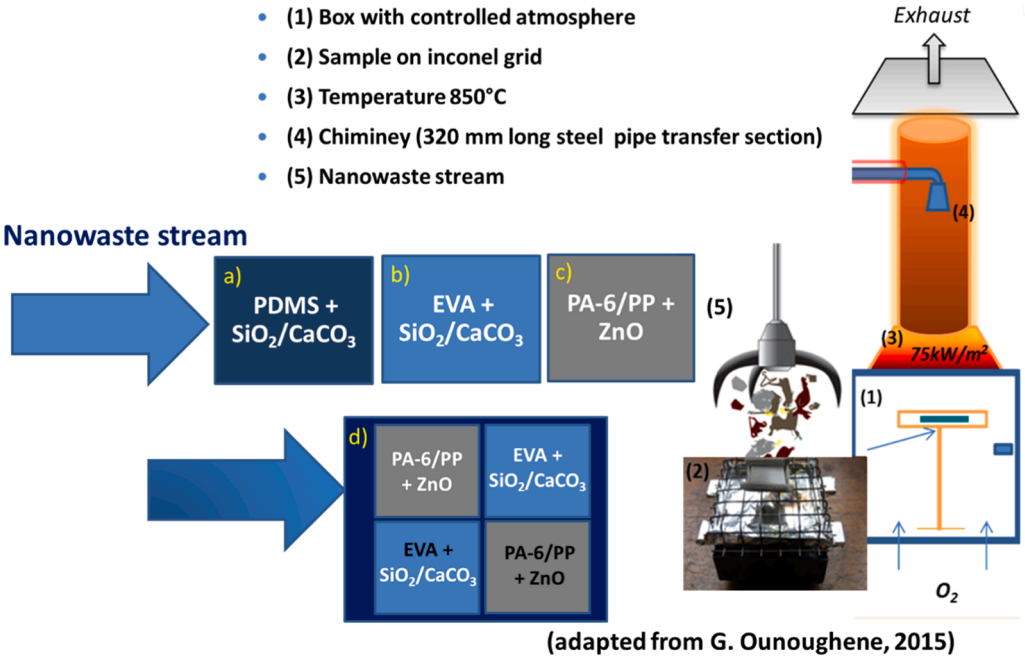

Fig. 1. Illustration of 4 nanowastes stream before incineration: a,b,c) individual nanocomposites and d) mixture nanocomposites simulation. Lab-scale incinerator (cone calorimeter with controlled atmosphere according to G. [23]).

Vulcanization, HTV) was provided by Elkem Silicones. The silica particles were purchased from Evonik (Aerosil 150 noted SiO_2) and the calcium carbonate (Socal 31 noted $CaCO_3$) was supplied by Solvay. SiO_2 used was a hydrophilic fumed silica with a specific surface area (BET value) of 135–165 m^2/g (data from manufacturer) and average primary particle size of 14 nm. $CaCO_3$ was an ultrafine precipitated calcium carbonate (particle diameter between 50 and 100 nm) with a specific surface area (BET value) of 17 m^2/g (data from manufacturer). Nanoparticles were selected and mixed in order to reproduce industrial formulations of the cable industry.

Polymer blend (PA-6/PP) was provided by Arkema (rigid Orgalloy®). PA-6/PP was chosen as a model of polymer blends to generate no residue after incineration step. ZnO has been widely used for the UV-stabilization in the field of automotive sector [26], and is a good candidate to promote a carbonaceous structure and create a pro-inflammatory response [25]. The zinc oxide nanopowder was purchased from Nanoshel.

2.2. Nanocomposites preparation

The silicone matrix, kindly supplied by Elkem Silicones, contained 74.4 wt% of vinyl-terminated polydimethylsiloxane (M_W of 550,000 g/mol) and 0.6 wt% of 2.5-dimethyl-2.5-di(tertbutylperoxy)hexane as a crosslinking agent. It was specifically prepared in order to avoid the presence of any other additives in the formula. Composite formulations were prepared using a HAAKE internal mixer at a temperature of 40°C, shear rate of 40 rpm and mixing time of 50 min. The HAAKE internal mixer has two rotors running in a contra-rotating way to blend the filler and matrix. Thereafter, filled silicone was crosslinked under heat at 150°C and with a pressure of 90 bars during 15 min to obtain a 10 cm×10 cm x 0.4 cm elastomer sheet.

EVA compound formulation was carried out *via* a twin-screw corotating (Clextral, BC21 type, France). This extruder has a 25 mm diameter screw profile, a 4 mm diameter die, and an L/D (length/diameter) ratio of 48. The extrusion temperature used was 170°C. The obtained pellets were injection moulded (Krauss Maffei 180-CX 50) to obtain sheets with similar dimensions. Two nanocomposites based on EVA or PDMS that are of relevance to cable industries applications were formulated by adding 40 % by weight nanofillers (mixture of $SiO_2/CaCO_3$; ratio 1:1). ZnO with a content fixed at 5 wt% (as inorganic UV filters) was dispersed in the polymer blend (PA-6/PP) by extrusion with a processing temperature from 200 °C to 240 °C.

2.3. Experimental set-up: incineration process to collect by-products (residues and soot)

Existing set-up (Lab-Scale incinerator developed in 2015 by Ounoughene et al. and validated in previous works [12,22])with a specific device including a modified cone calorimeter (FTT) with an irradiance of 75 kW/m^2, controlled atmosphere (21 % O_2) and air flow of 160 L/min has been used (Fig. 1) and. During the test, released soot were captured using a polycarbonate filter membrane (Isopore 0.2 μm GTTP - Merck Millipore) in the extraction chimney. The sampling was performed in order to collect a maximum of soot for all characterization. Residue was also collected on the inconel grid located in the incinerator chamber. The same operating conditions were applied for all incineration tests and for all samples.

2.4. Characterization methods of pristine nanoparticles, soot and residues

Physicochemical characterization of pristine nanoparticles and by-products generated after incineration process were conducted using several analytical techniques according to [27,28] required for nanotoxicology and risk assessment for nanomaterials.

Dimensional characterizations were performed by scanning electron microscopy (SEM) to assess particle size distribution, constitutive particle size and morphology; dynamic light scattering (DLS) to provide the intensity-averaged hydrodynamic diameter. Chemical identifications were performed by Energy-Dispersive X-Ray Spectroscopy EDS and Pyrolysis-Gas Chromatography coupled with Mass Spectrometry (Py-GC/MS) and zeta potential to access to the surface charge. Structural characterizations were achieved by using X-ray powder diffraction (XRD) for crystallinity structure and BET (Brunauer Emmett Teller) to assess specific surface area.

2.4.1. Scanning Electron Microscopy

SEM images were performed with a Zeiss ULTRA-Plus equipped with a Field Emission Gun (FEG) microscope and in-Lens SE detector. All images were carried out through secondary electrons collected by InLens detector. The size measurement was done on SEM images to measure a minimum number of 300 particles and obtain an average size that is representative of the sample. Platypus®, software developed by Pollen Metrology [29] allows the user to measure and automatically count particles by adjusting an ellipse on a particle. Then the particle edge and corresponding area inside the edge were automatically calculated. From images, the equivalent diameter, $D_{SEM\text{-}eq.}$, was determined, this measurand is defined as the diameter of a sphere that would have a projected surface similar to the projected image of nanoparticle to be measured.

The size distribution was estimated using the Maximum-Likelihood estimation statistical method. Prior to the calculation, a choice must be made regarding the theoretical probability distribution that is suitable to represent the size distribution [30]. Four theoretical models: Gaussian, Lognormal, Gaussian mixture, and Lognormal mixture, were used to draw the histograms. The probability density function (PFD) of the 4 models was determined for the measured sizes of the single particles. To discriminate between the 4 models, we used the Akaike Information Criteria (AIC) and the Bayesian Information Criteria (BIC). The best model is the one that has a minimum AIC and/or BIC, with the BIC criterion preferred in case of conflict (taking into account the complexity of the model and favouring the model with the fewest parameters). Dynamic Light Scattering (DLS)

Since DLS measurements must be performed in suspension, all the by-products' particles from filters (soot) or grids (residues) were extracted into deionized water. The hydrodynamic diameter of nanoparticles in each suspension was measured by DLS with a Zetasizer Nano ZS from Malvern equipped with a Helium-Neon laser (4 mW - 632.8 nm). DLS was used to obtain information about the hydrodynamic diameter of nanoparticles, the average size distribution (Z-average) and the dispersity index. Around 250 μL of sample were deposited onto the cell as dispersion and were irradiated by a laser. Each acquisition was processed by cumulates method.

2.4.2. Zeta potential

The optimal dispersion of nanoparticles on a substrate depends on zeta potential of the initial suspension. The nanoparticles are well dispersed when the suspension is stable and when absolute value of the zeta potential is higher than |30| mV. For each sample, the measurements of zeta potential as a function of pH were carried out by keeping constant ionic strength (1 mM) with sodium perchlorate solution, perchloric acid and sodium hydroxide of concentration 0.1 mol/L.

2.4.3. Specific surface area

The characterization of individual particles was performed by measuring average particle size, polydispersity index, and specific surface area using BET method that is expected to be a pertinent characteristic for ecological and toxicological hazard assessment. The equivalent diameter was calculated according to Wohlleben et al. Wohlleben et al., [31]. The equivalent primary particle diameter, d_{BET}, was calculated, by assuming a spherical shape of particles (see Eq. 1).

$$d_{BET} = 6000/(S_{BET} * \rho_{particle}), \quad (1)$$

where S_{BET} is the surface measured by BET and $\rho_{particle}$ corresponds to the particle density.

2.4.4. Pyrolysis-gas chromatography coupled with mass spectrometry

Py-GC/MS analysis was used for gases identification. Pyroprobe 5000 pyrolizer (CDS analytical) equipped with an electrically heated platinum filament was used to flash pyrolyze the samples in a helium environment. One coil probe enables the pyrolysis of samples (1 mg) placed in a quartz tube between two pieces of rock wool. The sample was heated at 900 °C and the temperature was held for 15 s, and then the gases were sent to the gas chromatograph for 5 min. The pyroprobe 5000 is inter-faced to a 450-GC chromatograph (Varian) by means of a chamber heated at 270 °C. In the oven, the initial temperature of 70 °C was raised to 310 °C at 10 °C/ min. The column is a Varian Vf-5 ms capillary column (30 m length; thickness = 0.25 mm) and helium (1 L/ min) was used as the carrier gas, a split ratio was set to 1:50. The gases were introduced from the GC transfer line to the ion trap analyser of the 240-MS mass spectrometer (Varian) through the direct-coupled capillary column.

2.4.5. X-Ray diffraction

XRD analyses of pristine particles and soot and residues were performed on a Bruker X-ray diffractometer using Cu K_α radiation.

2.5. In vitro toxicity assessment

Residues and soot in powder form were weighted and dispersed using ultrasonication in MilliQ water. The stock suspension was ultrasonicated by Bioblock Scientific Vibracell 75043 probe-sonicator (750 W, 20 HHz, 13 mm horn) with a dispersion energy value fixed at 1667 J/mL (amplitude of 40 %) combined with cycles of pulses (10 s ON, 10 s OFF) during 20 min in cooled external ice water bath according to previous work [32]. DMEM stock dispersions were prepared by diluting by-products in DMEM as described below.

2.5.1. Cell line and culture conditions

The RAW 264.7 cell line derived from murine peritoneal macrophages transformed by the Abelson Murine Leukemia Virus was provided by the ATCC Cell Biology Collection (Promochem LGC, Molsheim). Cells were cultured in Dulbecco's Modified Eagle's Medium (DMEM, Biowest), complemented with 10 % of foetal calf serum (FCS, Biowest), 1 % penicillin-streptomycin (penicillin 10 000 units/mL, streptomycin 10 mg/mL; Biowest) and incubated at 37°C under a 5 % CO_2 humidified atmosphere. Cell viability was determined by trypan blue dye exclusion. For each experiment, cells were seeded in 96-well plates (100 000 cells/well to assess Tumour Necrosis Factor alpha and reactive oxygen species production, and 25 000 cells/well for lactate dehydrogenase assays) in 25 µL of complete DMEM (DMEMc), as previously described [33,34]. Suspensions of nanoparticles were prepared at a concentration of 1200 µg/mL in water milliQ. For contact with cells, samples were further diluted in DMEMc to reach the following final concentrations: 11.25, 22.5, 45 and 90 µg/mL. The stability of the suspensions was checked (dynamic light scattering, nanozetasizer, Malvern instrument) and samples were added to the cell culture and incubated for 90 min or 24 h at 37 °C in a 5 % CO_2 humidified atmosphere. A negative control, corresponding to the cells incubated alone, was included. Three independent experiments were performed for each condition.

2.5.2. Cytotoxicity assays

After a 24 h incubation of cells with the samples, the activity of the lactate dehydrogenase (LDH) released from cells with damaged membranes was assessed in the culture supernatant. The CytoTox-ONE™ Homogeneous Membrane Integrity Assay (Promega, Charbonnières les bains, France) was used according to the manufacturer's instructions. Detection was performed using a fluorometer (Fluoroskan Ascent, Thermolabsystems), with excitation/emission wavelengths set at 530/ 590 nm. The activity of the released LDH was reported to that of negative control cells (unexposed to the samples). A positive control was also included and consisted of the total cellular LDH released (measured after the lysis of control cells).

2.5.3. Pro-inflammatory response

Tumour Necrosis Factor alpha (TNF-α) production was assessed in the cell culture supernatant after a 24 h contact between cells and samples. It was assessed using a commercial enzyme-linked immunosorbent assay (ELISA) kit (Quantikine® Mouse TNF-α Immunoassay, R&D Systems). The optical density of each well was determined according to the manufacturer's instructions by using a microplate reader (Multiskan RC, Thermolabsystems) set to 450 nm. A standard curve was established and results were expressed in picograms of TNF-α per millilitre of supernatant.

2.5.4. Oxidative stress

The OxiSelect™ ROS Assay Kit (Euromedex, Mundolsheim, France) was used to detect a large array of reactive oxygen species (ROS) activity. The assay uses the conversion of a non-fluorescent substrate, 2.7′-dichlorodihydrofluorescein diacetate that can easily diffuse through cell membranes and be converted into a fluorogenic molecule 2′.7′-dichlorodihydrofluorescein (DCF) in the presence of ROS. The fluorescence detected using a Fluoroskan Ascent fluorometer (Ex: 480 nm, Em: 530 nm, Thermolabsystems) is directly related to the ROS level. The production of ROS was assessed after 90 min (short term oxidative stress) and 24 h (long term oxidative stress) of cell/ sample contact and was expressed as nanomolar using a standard curve previously established.

3. Results

3.1. Physicochemical characterization of pristine nanoparticles

SEM images (Fig. S1) were used as a direct method to define the morphology and to perform the dimensional characterization of pristine $CaCO_3$ and SiO_2 nanoparticles.

For the pristine nanomaterials, the mean equivalent diameter was obtained by SEM measurement by assuming spherical particles, $D_{SEM\text{-}eq.}$ for SiO_2 and $CaCO_3$ were 14.3 ± 4.3 nm and 89.6 ± 25 nm respectively. To complete the dimensional characterisation of nanoparticles surface specific area in powder form of nanoparticles have been evaluated by BET [31]. Specific surface area of SiO_2 and $CaCO_3$ were 150 and 23 m^2/g respectively (corresponding to an equivalent diameter of 15.1 nm for SiO_2 and 96.3 nm for $CaCO_3$ by assuming spherical particles model described Eq. 1). Values are consistent with constitutive SEM nanoparticles analysis with 15 nm for SiO_2 *vs.* 14 nm by SEM and 96 nm for $CaCO_3$ *vs.* 90 nm by SEM.

The particles surface charge can vary from one nanoparticle to another, depending on the elements present at the surface and has a direct impact on the zeta potential value. It is therefore an indirect way to identify the state of agglomeration/aggregation. The surface charge of SiO_2 and $CaCO_3$ nanoparticles was evaluated by zeta potential measurement. The nanoparticles are negatively charged $\zeta_{SiO_2} = -34.6$ mV and ζ_{CaCO_3} =-5.5 mV. A negative zeta potential was also measured for the physical mixture of $SiO_2/CaCO_3$ (1:1) ($\zeta_{SiO_2/CaCO_3}$ =-22 mV). To go in depth, the hydrodynamic diameter was measured by DLS to evaluate the state of agglomeration/aggregation of SiO_2 and $CaCO_3$ at neutral pH. Silica nanoparticles presented a *Z-average* equal to 156.6 nm as measured by DLS, corresponding to the size of agglomerates/aggregates observed by SEM. Consequently, the DLS and SEM measurements are consistent. $CaCO_3$ nanoparticles aggregates measured by DLS presented a *Z-average* equal to 521.8 nm. The physical mixture of $SiO_2/CaCO_3$ (1:1) presented an average agglomeration/aggregation size with a *Z-*

Table 1
Summary of the physicochemical features of the SiO_2 and $CaCO_3$ nanoparticles.

	Parameters analysed	SiO_2	$CaCO_3$
SEM	Mean diameter (nm)	14.3	89.6
	Shape	Pseudo-spherical	Irregularly rhombohedral
XRD	Amorphous or crystalline structure	Crystalline structure	Crystalline structure
BET	Specific surface (m^2/g)	150	23
DLS	Hydrodynamic diameter (nm)	156.6	521.8
Surface charge	Zeta potential at natural pH (mV)	- 34.6	- 5.5

average equal to 289.5 nm. Table 1 summarizes the main physicochemical features of SiO_2 and $CaCO_3$ before incorporation in PDMS or EVA polymer.

3.2. Physicochemical and morphological transformation of nanoparticles in soot and residues after incineration of EVA and PDMS nanocomposites

3.2.1. Dimensional characterisations of constitutive nanoparticles in soot and residues

Fig. 2 shows SEM images to visualize the fate of nanoparticles mixture, $SiO_2/CaCO_3$, (in soot and/or residue) after incineration of EVA or PDMS based nanocomposites (Fig. 2a, b).

In the case of incineration of the EVA matrix in absence of nanoparticles, only soot was generated as end-products due to the total degradation of the polymer over 450 °C (and thus we observed the

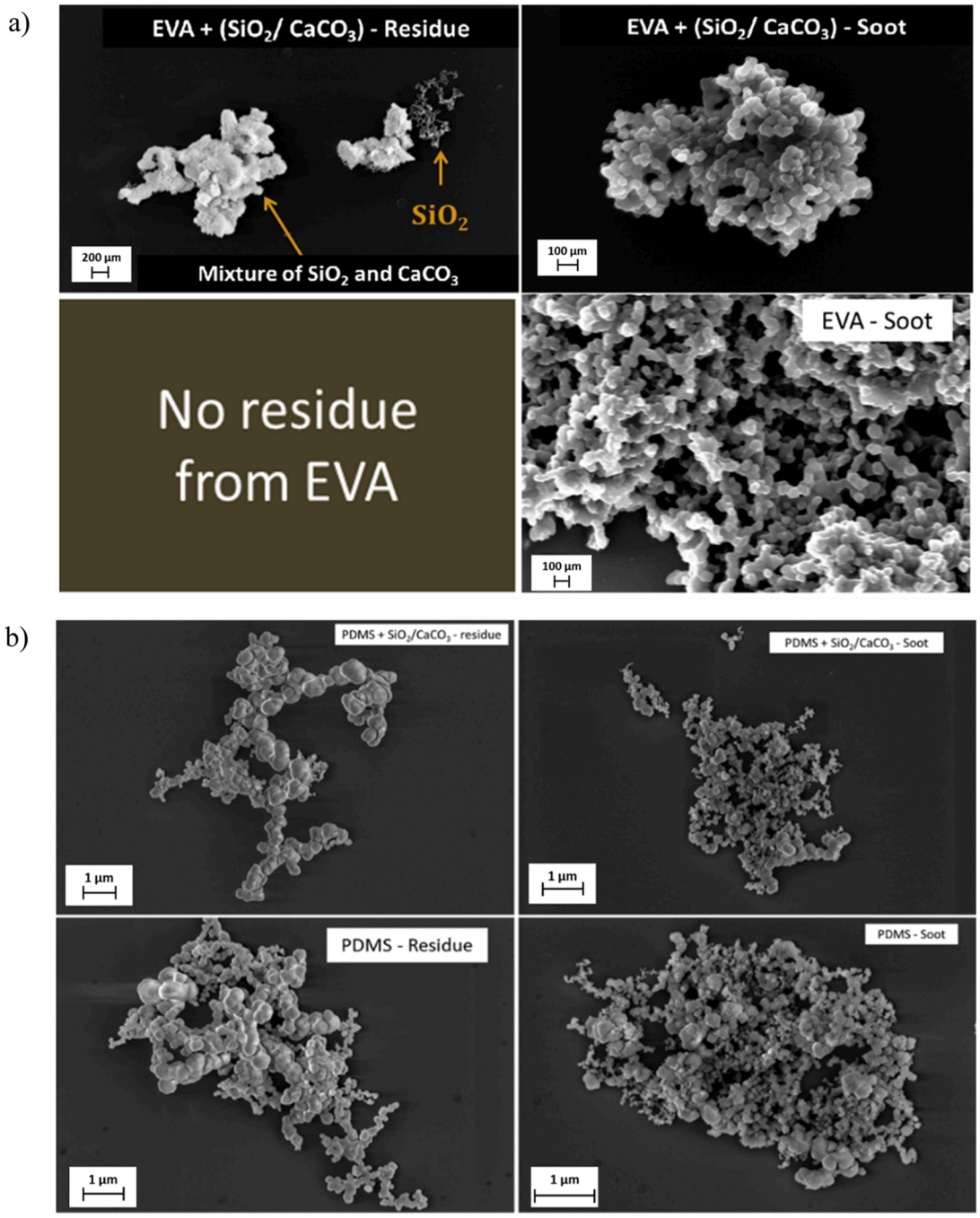

Fig. 2. SEM images from soot and residue after incineration process of EVA (a) and PDMS (b) pristine polymers and based nanocomposites.

Table 2
Statistical parameters from SEM measurement (average diameters and standard deviation of the size distribution).

Measurand Samples	$D_{SEM\text{-}eq}$ (nm)	Standard deviation of the size distribution
Incineration of the polymer matrix		
EVA - Soot	63.6	15.4
EVA - Residue	None	None
PDMS - Soot	54.2	42.5
PDMS - Residue	174.1	89.1
Incineration of nanocomposites soot and residues		
EVA + (SiO_2/$CaCO_3$) - Soot	54.9	14.9
EVA + (SiO_2/$CaCO_3$) - Residue	19.1	7.3
PDMS + (SiO_2/$CaCO_3$) - Soot	71.7	42.2
PDMS + (SiO_2/$CaCO_3$) - Residue	100.3	50.4

absence of residues). The soot morphology from EVA-based nanocomposite appeared quite similar to the soot generated by the incineration of the pristine EVA matrix (without SiO_2/$CaCO_3$ nanoparticles). Thus, the presence of SiO_2/$CaCO_3$ did not seem to affect the structure of the soot of EVA nanocomposite compared to the soot provided by pristine EVA matrix. In both cases the soot consisted of a charred and agglomerated structure of pseudo-spherical nanoparticles. For EVA nanocomposite and pristine EVA, the dimensional soot were around 55 nm and 64 nm, respectively.

By contrast, the addition of SiO_2/$CaCO_3$ nanoparticles clearly changed the thermal degradation pathway of the EVA polymer matrix since a residue was produced (residue which was absent for the incineration of the EVA matrix without nanoparticles). Concerning the PDMS matrix, both soot and residues were generated as observed in a previous work [22]. The presence of the SiO_2/$CaCO_3$ nanoparticles did not seem to modify the morphology of both by-products (soot and residue). The primary particles provided from PDMS matrix presented a size diameter around 54 nm for the soot and 174 nm for the residues with an observable phenomenon of aggregation/agglomeration.

The nanocomposites formulation using a mixture of SiO_2/$CaCO_3$ nanoparticles in EVA or PDMS can induce physicochemical reactions (synergistic or antagonistic) and size modifications of released primary nanoparticles. The addition of nanoparticles in PDMS seemed to affect the residue by favouring the agglomeration/aggregation phenomena giving an average particle size around 100 nm. On the opposite, the soot size seemed less impacted by the presence of SiO_2/$CaCO_3$ nanoparticles.

From the SEM images, a set of particles of each type of nanowaste was measured in order to construct a histogram of number size distribution (Fig. S2). Primary particle was measured as recommended by the European authorities. In order to ensure that the dimensional measurements are representative of the entire population studied, around 300 particles were analysed by using Platypus software [29]. For each set of data, the number size distribution was constructed (Fig. S2) and different parameters were extracted (average diameter and standard deviation of the size distribution) (Table 2).

3.2.2. *Surface charge measurements and aggregation/agglomeration phenomena*

Fig. 3 shows the evolution of the zeta potential (*ZP*) with the pH value for each sample. For the pristine nanoparticles alone, the evolution of zeta potential depends on the nanoparticle's chemistry. So, the ratio 1:1 of nanoparticles mixture led to an intermediate evolution. Concerning the soot, the zeta potential was not significantly affected by the presence of the nanoparticle mixture as shown by comparing the zeta potential of pristine matrices (PDMS or EVA) and that of the nanocomposites. No residue was obtained from thermal degradation of EVA matrix. For PDMS residues, the evolution of the zeta potential was very close for pristine and filled matrices.

The hydrodynamic diameter for SiO_2/$CaCO_3$-nanoparticle mixture was evaluated at 289.5 nm corresponding to an average value of pristine nanoparticles. The hydrodynamic diameter from matrices soot increased

Table 3
Summary of the evaluation of the agglomeration/aggregation state before and after the incineration process.

Measurand Sample	*Z-average* (nm)	*ZP* (mV) @ initial pH
Pristine nanoparticles		
SiO_2	156.6	−34.6
$CaCO_3$	521.8	−5.5
Physical mixture SiO_2/$CaCO_3$ (1:1)	289.5	−22
Incineration of the polymer matrix		
EVA - Soot	345.1	−35
EVA - Residue	*No residue*	
PDMS - Soot	197.3	−51.0
PDMS - Residue	792.1	−54.3
Incineration of nanocomposites soot and residues		
EVA + (SiO_2/$CaCO_3$) - Soot	204.6	−49.6
EVA + (SiO_2/$CaCO_3$) - Residue	211.2	−18.7
PDMS + (SiO_2/$CaCO_3$) - Soot	175.5	−51.3
PDMS + (SiO_2/$CaCO_3$) - Residue	1383.0	−47.2

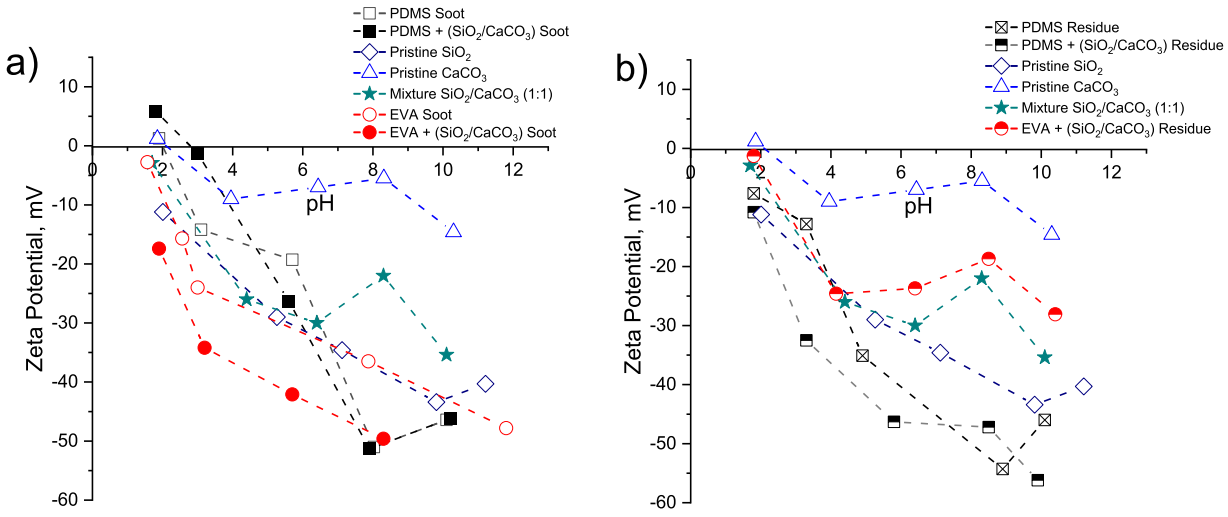

Fig. 3. Variation of zeta potential as a function of pH reported for a nanoparticle mixture (SiO_2/$CaCO_3$) (a) soot and (b) residue from EVA or PDMS based nanocomposites.

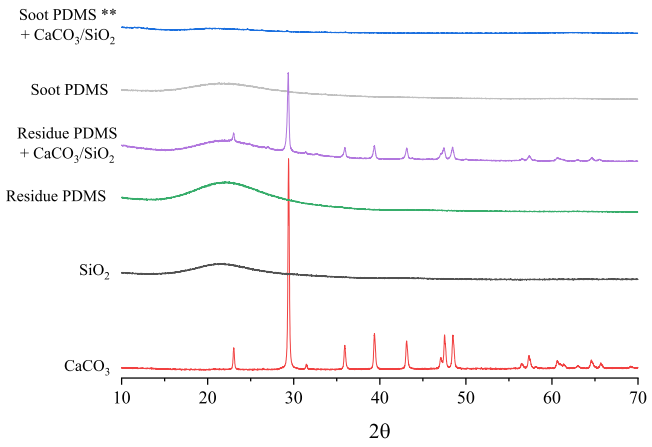

Fig. 4. XRD Pattern of samples based on PDMS. ** Soot PDMS + $CaCO_3/SiO_2$ analysed appeared less in intensity due to a fewer quantity of soot.

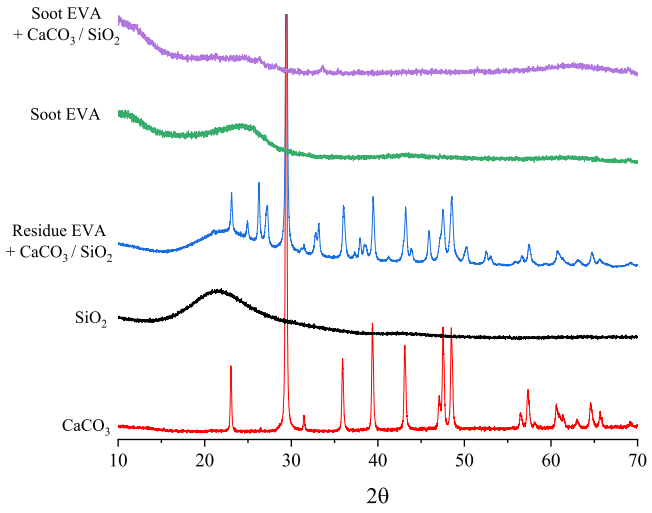

Fig. 5. XRD Pattern of samples based on EVA.

significantly corresponding to a phenomenon of agglomeration/ aggregation knowing that the primary nanoparticle soot value was respectively 64 nm for EVA and 54 nm for PDMS.

In soot, whatever the matrix, the presence of the nanoparticle mixture induced a decrease of the particle soot size hydrodynamic diameter. As the EVA matrix did not induce residues, the addition of nanoparticles generated particles agglomeration/aggregation with an equivalent hydrodynamic diameter close to those obtained by physical mixture of $SiO_2/CaCO_3$ (211 nm vs 289 nm respectively). In the PDMS + ($SiO_2/CaCO_3$) residue, the value of the hydrodynamic diameter was drastically increased. Table 3 summarizes the DLS measurements and the corresponding zeta potential (*ZP*) values.

3.2.3. *X-Rays diffraction analyses*

XRD analyses (Figs. 4 and 5) confirmed that there were detectable $CaCO_3$ particles inside the residues. $CaCO_3$ begins to decompose in CaO from 800°C [35], but re-carbonatation occurs afterwards, during the cooling phase, leading to transformation of CaO into $CaCO_3$. The presence of new diffraction peaks for both filled EVA and PDMS residues (*2θ* ~26/28°) indicates that re-carbonatation corresponds to the formation of calcite but also aragonite and vaterite which are allotropic varieties of $CaCO_3$. Silica entails the formation of a bump on all diffractograms. PDMS residues show the presence of a bump, even for pristine PDMS since an additional formation of silica results from the decomposition of the polymer in presence of oxygen.

3.2.4. *Analyses of released gases from thermal degradation*

To go in depth in the understanding of PDMS degradation, a Py-GC/MS analyse was carried out and allowed the gas released during the polymer degradation to be characterized.

PDMS and PDMS nanocomposite chromatograms (Fig. 6) showed a similar thermal degradation pathway. The only difference which could be highlighted was the size of the cyclosiloxanes generated. Concerning the PDMS chromatogram the identified cycles were comprised of 3 units to more than 10 units, unlike for PDMS nanocomposite where the cycles were limited to around 6 units. These results were consistent with the literature [36].

Concerning EVA chromatogram (Fig. 7), the peaks present between 5 min to 25 min correspond to alkanes and alkenes generated by the degradation of the macromolecular skeleton. The comparison of both EVA's formulations chromatograms showed a modification of the released gas proportions during the pyrolysis in the presence of the $SiO_2/CaCO_3$ mixture. Indeed, the presence of the nanoparticle mixture exacerbated the peaks corresponding to the release of benzene (2.94 min), toluene (4.03 min), styrene (5.24 min), indene (8.52 min) and naphthalene (10.97 min). The nanoparticles mixture seemed to induce a thermal degradation pathway favouring aromatic structures, these types of structure being at the origin of soot and char formation.

3.2.5. *Elemental analysis of the by-products*

To explore the fate of the element of interest contained in the by-products, an elemental analysis was performed on the agglomerates/ aggregates using the EDS technique. For all samples, we analysed the impact of the nanoparticle mixture ($SiO_2/CaCO_3$) on the by-products by using a deposit on a Cu-grid that allowed us to quantify the Si element instead of silica wafer usually used.

The proportion in the by-products of the following elements of interest: Si, Ca, C and O can be estimated from EDS spectrum and the particles partitioning was scrutinized and the state of agglomeration/ aggregation was evaluated after incineration process (Figs. 8 and 9).

Concerning the EVA nanocomposite soot, noticeable amounts of carbon were found. The release of inorganic nanoparticles SiO_2 and $CaCO_3$ in soot was not obviously observed during incineration of EVA nanocomposite.

The relative abundance of Si elements in PDMS soot suggested that the particles were made only of silicon dioxide (SiO_2). Silica could come from PDMS and nano-silica incorporated in the nanocomposite. The $CaCO_3$ was located in residue and not detectable in soot. The simultaneous presence of silicon and absence of calcium in the soot tends to confirm that most of the nanoparticles found in the aerosol were mainly generated by the PDMS degradation and to a lower impact of the silica initially introduced in the PDMS nanocomposite.

Experiments revealed significant amounts of $CaCO_3$-nano-nanoparticles in the residues of EVA nanocomposite and a very low presence of Si element. Results are in accordance with XRD analyses where some silicon dioxide was observed in residue whereas the signature of calcium carbonate was clearly noticed.

The observation of the repartition of silicon, oxygen and calcium in the PDMS residue (Fig. 9) allowed to conclude that the presence of silica seemed significant. As already mentioned, silica is issued from both PDMS degradation owing to oxidant degradation atmosphere and from the silica initially introduced in the nanocomposite. The analyse of PDMS residue highlighted information on the fate of silica particles, with the formation of particles mainly higher than 100 nm. In the residues of PDMS nanocomposite, as indicated by the size distribution of particles, only medium (~ 50 nm) and bigger (> 100 nm) size of nanoparticles were measured. The analysis of all the elements of interest by EDS highlighted some traces of Ca and suggested that the main degradation products coming from PDMS was silica. Moreover, EDS also showed the presence of carbon which could be ascribed to silicon

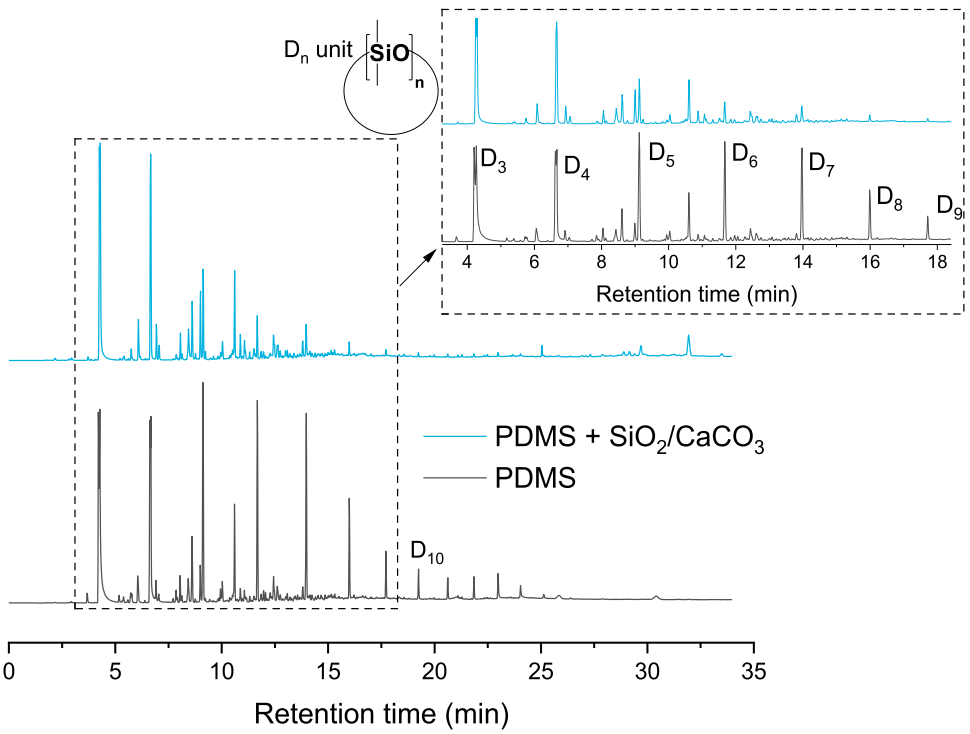

Fig. 6. Chromatograms obtained by Pyrolysis GC/MS of PDMS and PDMS nanocomposite.

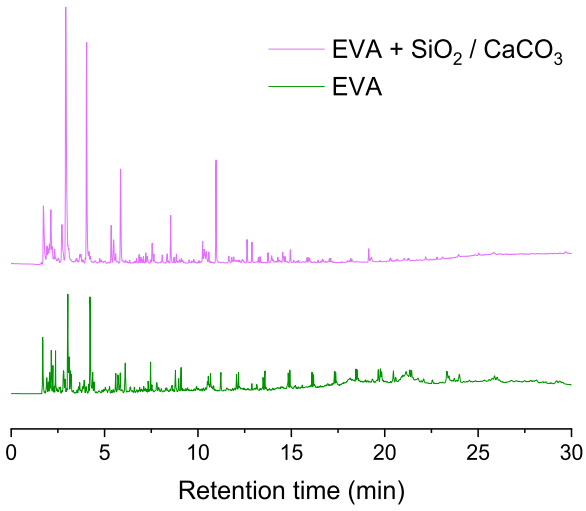

Fig. 7. Chromatograms obtained by Pyrolysis GC/MS of EVA and EVA nanocomposite.

oxycarbide formation ($Si_xO_yC_z$) [22].

Fig. 11 illustrates the presence of silicon and oxygen which correspond exactly to the location of the particles. This clearly confirmed the presence of silicon dioxide particles in PDMS based nanocomposite residue. In addition, the presence of calcium enabled to confirm that calcium carbonate was also mainly present in the EVA based nanocomposite residue.

3.2.6. Simulation of a waste stream composed by a mixture of nanoparticles (SiO_2 and $CaCO_3$) incorporated in an EVA and a blend polymer matrix (PA-6/PP) with ZnO in order to determine their release and by-products distribution in soot or residue ash

To further investigate a residual ash and soot formed during the incineration, observation of particles was conducted by EDS.

In a previous paper [25], we studied the effects of another type of commonly used nanocomposite: PA-6/PP+ZnO. Then we combined this nanocomposite to that studied in the present paper to mimic the incineration of a mixture of nanocomposites as can happen in real life with the aim of determining which component governs the toxicity of the incineration by-products. Fig. 10 shows the by-products obtained after incineration of the nanocomposites PA-6/PP and the mixture of nanocomposites.

The partitioning of nanoparticles in the by-products obtained after the incineration of the mixture (EVA-SiO_2/$CaCO_3$ and PA-6/PP-ZnO) (50/50) are reported in Figs. S3 and S4 respectively for soot and residual ash.

3.3. Toxicological profile of the nanowastes resulting from EVA or PDMS nanocomposites incineration

3.3.1. Cytotoxicity

The results of the LDH release assay, corresponding to cell membrane damage and thus the cytotoxicity induced, are reported in Fig. 11.

Pristine SiO_2 nanoparticles exhibited a moderate dose-dependent toxicity, with a significantly different LDH level compared to the negative control (cells incubated without nanoparticles) only at the highest concentrations. By contrast, pristine $CaCO_3$ nanoparticles were not cytotoxic at all. Finally, the SiO_2/$CaCO_3$ mixture did not induce a significant toxicity. However, we can convert the dose effect of SiO_2/$CaCO_3$ mixture to SiO_2 dose effect considering the weight ratio 1:1 for the nanoparticle's mixture composition. Indeed, the mixture dose effect at 90 μg/mL is equivalent to the dose effect of SiO_2 at 45 μg/mL. So, it is not as SiO_2/$CaCO_3$ mixture is biologically inert but as for the weight ratio 1:1 the dose effect is divided by 2. In other words, for the cytotoxicity profile of SiO_2/$CaCO_3$ mixture, the dose effect appears too low to induce a cytotoxic response considering that SiO_2 alone already presents a moderate response.

The PDMS residue induced a dose-dependent toxicity and presented a similar pattern with or without the nanoparticle mixture. Same conclusion could be drawn for the soot. This phenomenon can be explained by the chemical nature from thermal degradation by-

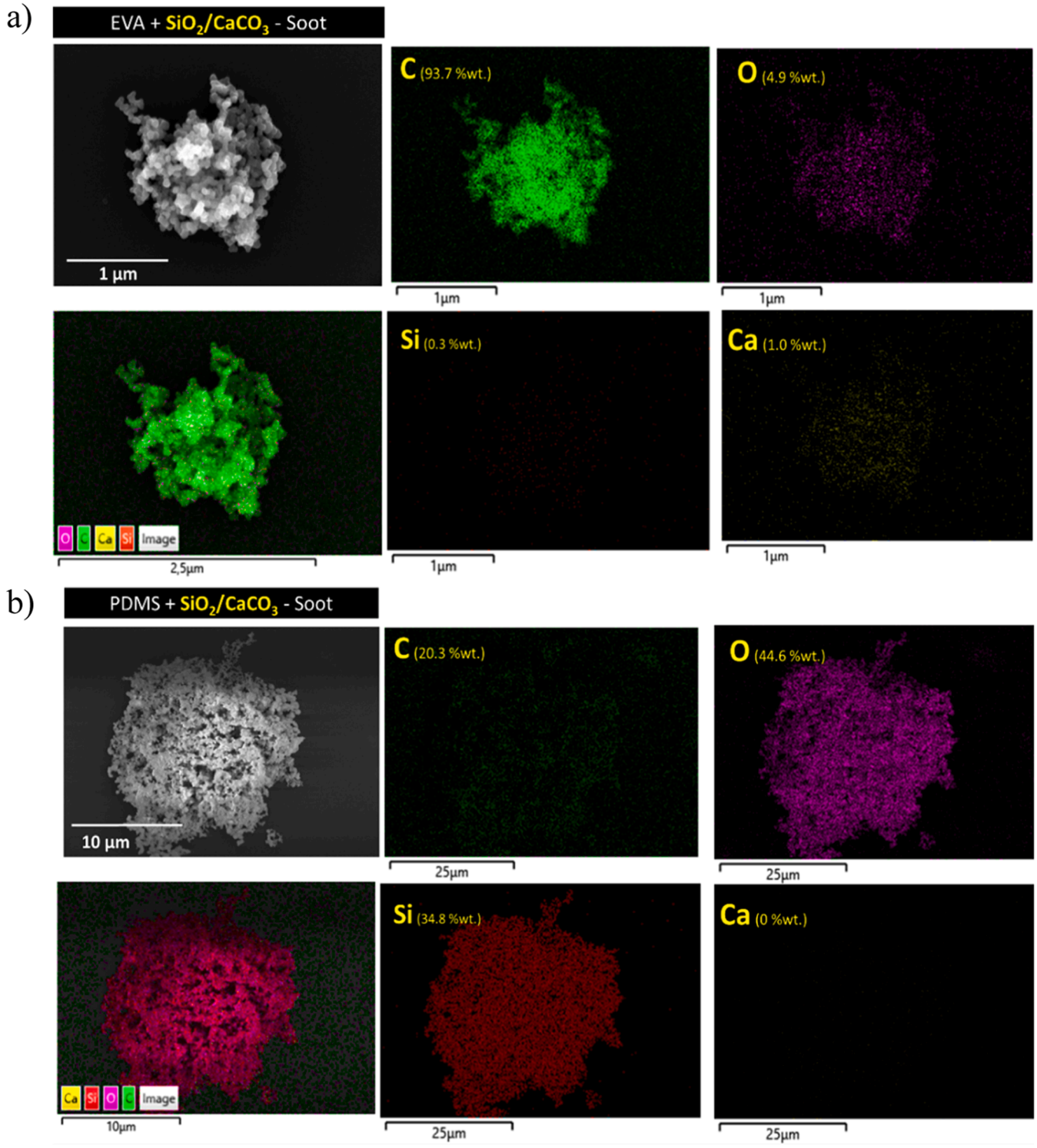

Fig. 8. EDS mapping and spectrum of soot nanocomposite with allocation and proportion of Si and Ca in the residual structure (a) EVA + $SiO_2/CaCO_3$ and (b) PDMS + $SiO_2/CaCO_3$.

products. Indeed, the PDMS generates silica nanoparticles, and the behaviour of these nanoparticles is equivalent to the introduced SiO_2 nanoparticles in polymer matrices. While EVA soot was not cytotoxic, EVA + $SiO_2/CaCO_3$ soot showed a dose-dependent toxicity, significant only at the highest concentration. On the contrary, EVA + $SiO_2/CaCO_3$ residue was not cytotoxic.

3.3.2. *Pro-inflammatory response*

The results of the production of TNF-α, a major pro-inflammatory cytokine, are reported in Fig. 12.

All samples were able to induce a dose-dependent pro-inflammatory response, especially at high concentrations. Pristine SiO_2 and $CaCO_3$ showed a quite similar pro-inflammatory behaviour, and their mixture induced a slightly higher response. Indeed, for the mixture of particles, additive effects are observed (no synergistic or antagonistic effect) as the

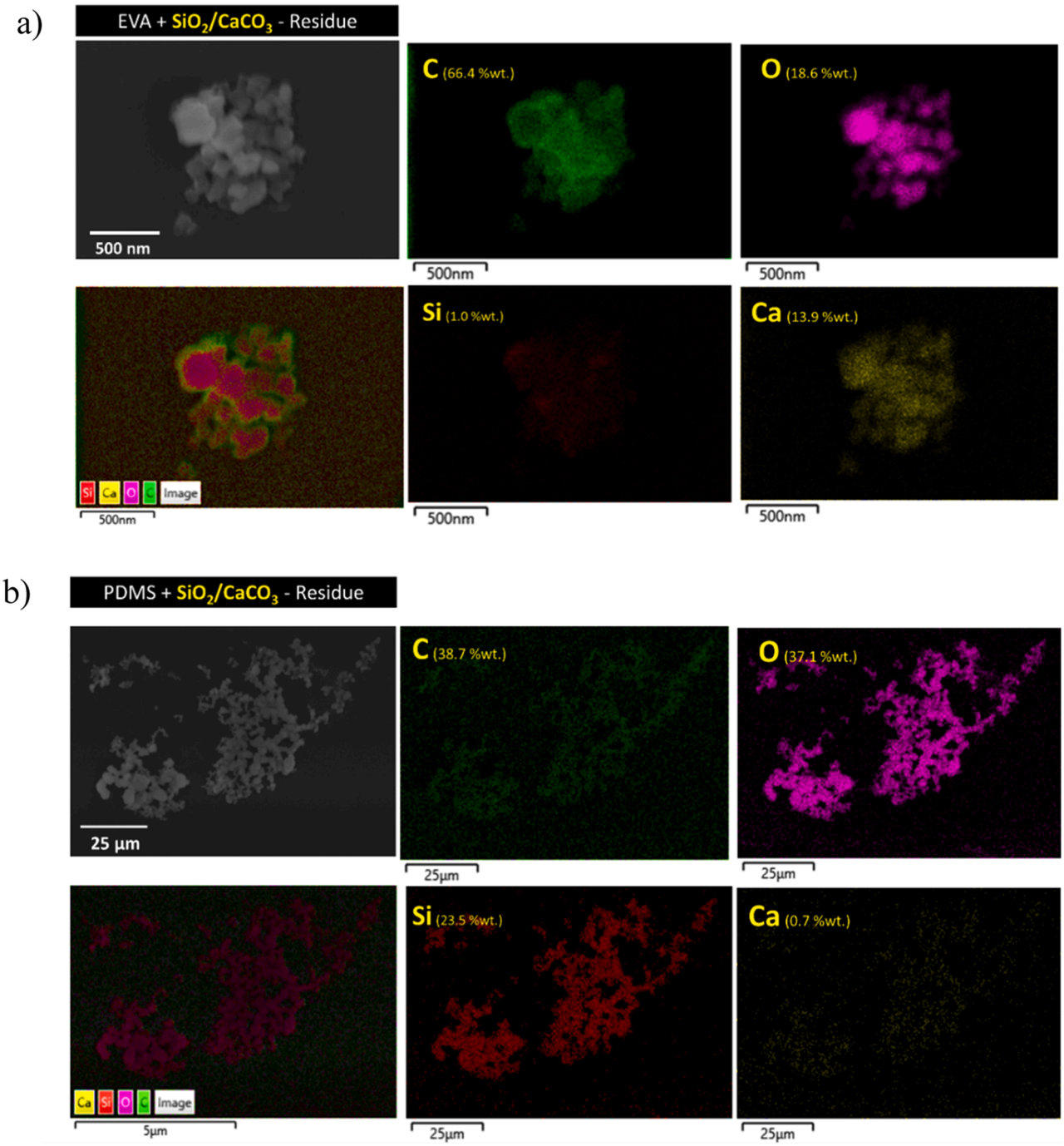

Fig. 9. EDS mapping and spectrum of residue nanocomposite with allocation and proportion of Si and Ca in the residual structure (a) EVA + $SiO_2/CaCO_3$ and (b) PDMS + $SiO_2/CaCO_3$.

response to 90 µg/ mL for $SiO_2/CaCO_3$ corresponded to the sum of the SiO_2 response at 45 µg/mL plus that of $CaCO_3$ at 45 µg/mL, considering the weight ratio 1:1 for the nanoparticle's mixture composition.

PDMS matrix without nanoparticles showed a slightly enhanced production of TNF-α in the residue compared to the soot. The pro-inflammatory response induced by PDMS matrix in the presence or in the absence of the $SiO_2/CaCO_3$ mixture was similar both at the level of residue and soot. EVA matrix filled with nanoparticles showed an enhanced production of TNF-α in the residue compared to the soot. The pro-inflammatory response induced by EVA + $SiO_2/CaCO_3$ soot was decreased compared to that observed for EVA soot. The comparison of the obtained results in cytotoxicity and pro-inflammatory tests showed that the LDH release is the more discriminant toxicity test. Indeed, all the samples had a pro-inflammatory response, however only a part of samples showed LDH release.

3.3.3. *Reactive Oxygen Species (ROS) production*

The production of ROS, indicative of the induction of oxidative stress, is reported in Fig. 13. No significant ROS production was observed, whatever the sample and the time of analysis.

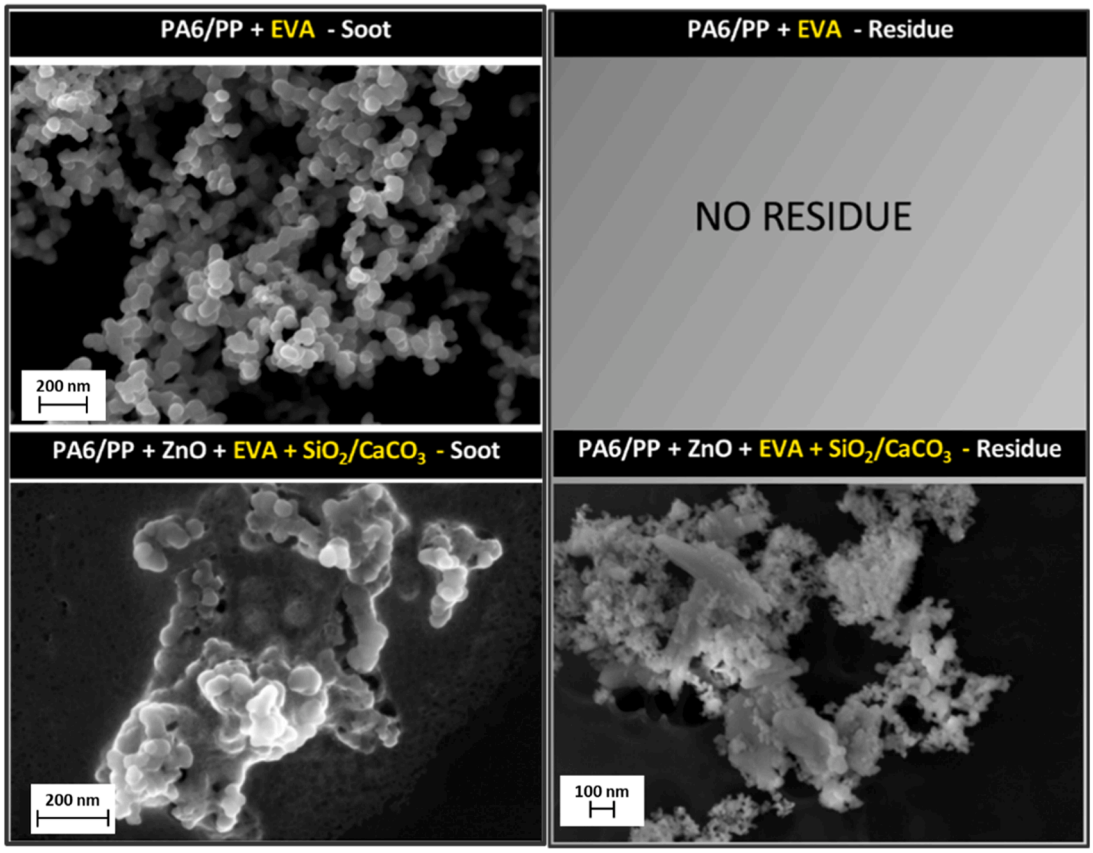

Fig. 10. Illustrations of by-products obtained after the incineration of the mixture (EVA-$SiO_2/CaCO_3$ and PA-6/PP-ZnO) (50/50).

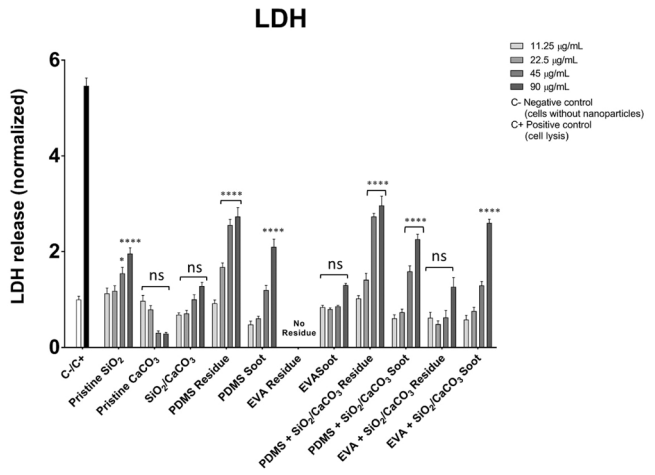

Fig. 11. Cytotoxicity of silica and calcium carbonate as fillers alone and by-products from PDMS and EVA nanocomposites as determined by the LDH release. Results are expressed relative to control (unexposed cells). Statistically different from control cells ****$p < 0.0001$, ***$p < 0.001$.

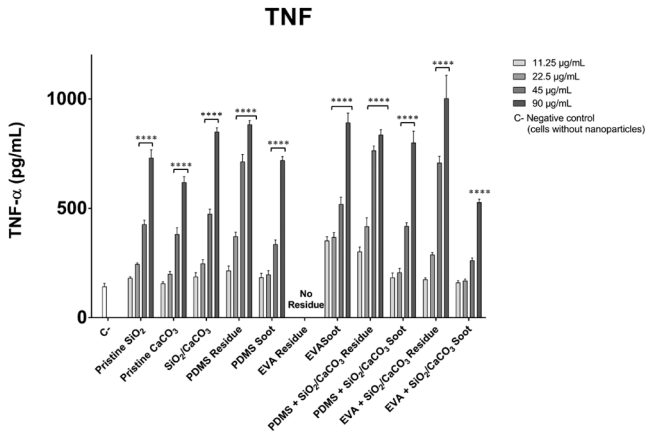

Fig. 12. Pro-inflammatory response induced by silica and calcium carbonate as fillers alone and by-products from PDMS and EVA nanocomposites as determined by the production of TNF-α. Results are expressed relative to control (unexposed).

3.4. Toxicological profile of the by-products obtained after incineration of complex mixture of 2 matrices and 3 nanofillers: EVA- $SiO_2/CaCO_3$ + PA-6/PP-ZnO

We assessed the toxicity of the by-products obtained after the incineration of a complex mixture made of 50 % EVA- $SiO_2/CaCO_3$ and 50 % PA-6/PP-ZnO.

The cytotoxicity, pro-inflammatory effects and oxidative stress induced by the by-products obtained after the incineration of the EVA-$SiO_2/CaCO_3$ and PA-6/PP-ZnO mixture are reported in Figs. S7, S8 and S9 respectively. For comparison, the toxicological profile of the pristine nanoparticles and that of the by-products of the nanocomposites are also represented.

To analyse the results, we have to keep in mind that the EVA-$SiO_2/CaCO_3$ + PA-6/PP-ZnO mixture is composed of half EVA-$SiO_2/CaCO_3$ and half PA-6/PP-ZnO, therefore when comparing the toxicological response of their by-products to that of the by-products of the individual nanocomposites, we should not make comparison at a similar dose but we should compare the toxicity of the mix at a certain dose to that of the

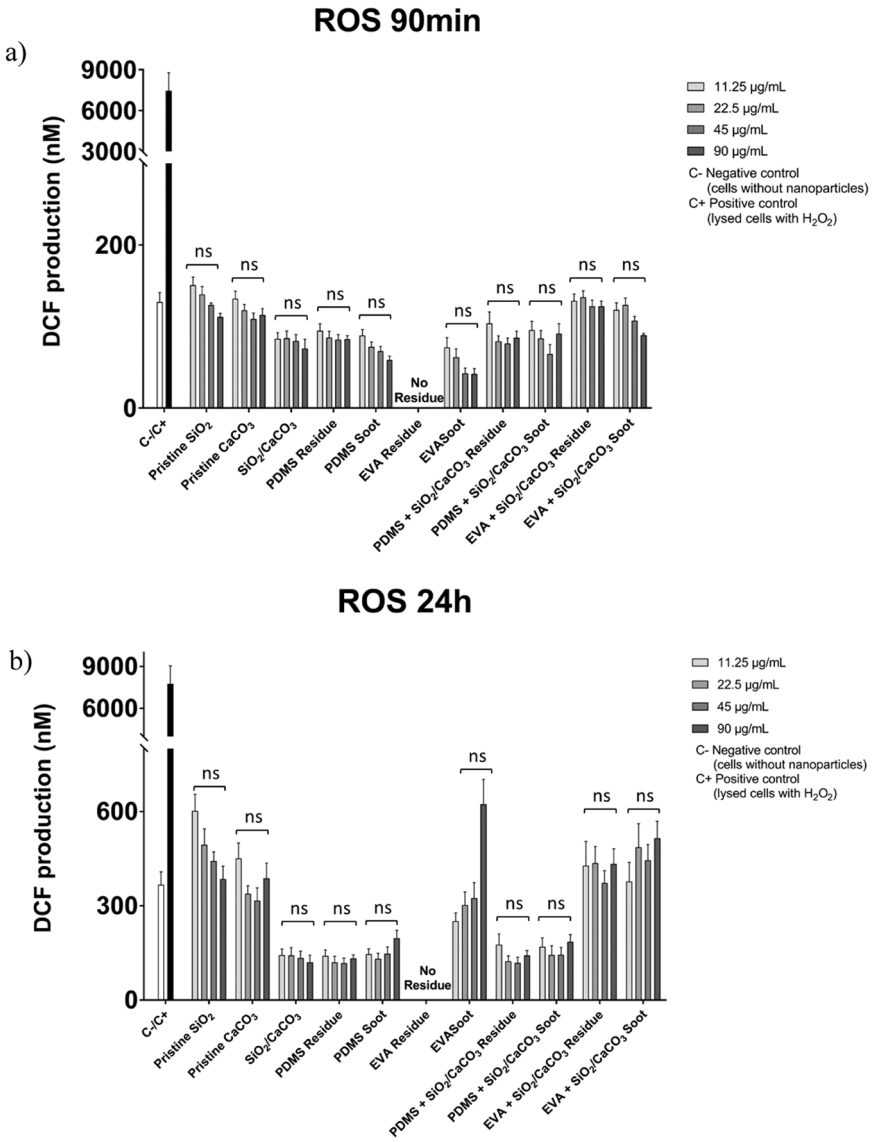

Fig. 13. Oxidative stress induced by silica and calcium carbonate as fillers alone and by-products from PDMS and EVA nanocomposites as determined by the production of ROS after 90 min (a) and 24 h (b) of cell-sample contact. Results are expressed relative to control (unexposed) cells. Statistically different from control cells $^{****}p < 0.0001$, $^{***}p < 0.001$, $^{*}p < 0.05$.

individual components at half this dose. For example, the effects of EVA- $SiO_2/CaCO_3$ + PA-6/PP-ZnO at 90 µg/mL should be compared to those of EVA-$SiO_2/CaCO_3$ or those of PA-6/PP-ZnO at 45 µg/mL. Keeping this in mind, we can make the following observations:

- The EVA- $SiO_2/CaCO_3$ + PA-6/PP-ZnO residue does not induce a significant toxicity compared to the control (unexposed) cells. Globally, we observe additive effects as the cytotoxic signal induced by the EVA- $SiO_2/CaCO_3$ + PA-6/PP-ZnO residue corresponds roughly to the sum of the cytotoxic effects of EVA- $SiO_2/CaCO_3$ residue and that of PA-6/PP-ZnO residue.
- The EVA- $SiO_2/CaCO_3$ + PA-6/PP-ZnO soot induces a significantly increased toxicity compared to control cells at the highest dose. As for EVA- $SiO_2/CaCO_3$ + PA-6/PP-ZnO residue, the effects were found to be additive, except at the highest concentration. By comparing the cytotoxic profile of EVA- $SiO_2/CaCO_3$ + PA-6/PP-ZnO soot to that of EVA- $SiO_2/CaCO_3$ soot, PA-6/PP-ZnO soot and pristine nanofillers, we can conclude that the toxicity triggered by EVA- $SiO_2/CaCO_3$ + PA-6/PP-ZnO soot is governed by SiO_2.

Regarding the pro-inflammatory effect induced by EVA- $SiO_2/CaCO_3$ + PA-6/PP-ZnO residue, we observe additive effects of EVA- $SiO_2/CaCO_3$ residue and PA-6/PP-ZnO residue only at the lowest concentration. As all components show a pro-inflammatory effect, it is impossible to determine which one governs the pro-inflammatory effect of EVA- $SiO_2/CaCO_3$ + PA-6/PP-ZnO residue. On the other hand, for EVA- $SiO_2/CaCO_3$ + PA-6/PP-ZnO soot, additive effects of EVA- $SiO_2/CaCO_3$ soot and PA-6/PP-ZnO soot are observed and it can be established that the pro-inflammatory effect is governed by the $SiO_2/CaCO_3$ nanoparticles.

Regarding oxidative stress, the EVA- $SiO_2/CaCO_3$ + PA-6/PP-ZnO by-products (both residue and soot) did not trigger an enhanced ROS production, whatever the time of analysis (90 min or 24 h).

4. Discussion

4.1. Fate of nanoparticles in different types of nanowaste stream after incineration (partitioning and physicochemical transformation)

The impact of the nanoparticle mixture ($SiO_2/CaCO_3$) on the released particles physicochemical characteristics was evaluated during

Table 4
Fate of nanoparticles elements from end by-products during incineration SiO_2/$CaCO_3$ nanocomposite-based EVA or PDMS.

		Incineration	
Matrix	**Initial nanoparticles**	**Soot**	**Residue**
EVA	-	Carbon	No residue
EVA nanocomposite	SiO_2 / $CaCO_3$	Carbon	Carbon, Oxygen and Calcium - Few Silicon
PDMS	-	Silicon	Silicon
PDMS nanocomposite	SiO_2 / $CaCO_3$	Oxygen, Silicon, Carbon	Carbon, Oxygen, Silicon, Calcium

the incineration process of PMDS or EVA based nanocomposites. Table 4 summarizes the main chemical composition of the matrices and nanocomposites after incineration provided by EDS mapping in Fig. S5 and S6.

Significant differences were observed about size distribution (soot and residue) between the pristine and filled matrices. According to the Py-GC/MS analyses, DLS measurements and SEM/EDS characterizations, in the case of EVA nanocomposite, the nanoparticles presence seemed to favour the formation of a carbonaceous structure during the incineration (residue). An intermediate structure (CaO) was formed that will be recarbonated during the cooling phase. Concerning the EVA nanocomposite, the individual particle size in the residue was directly induced by the silica and the calcium carbonate particles size with primary particle size at 19.1 nm. Moreover, the Zeta potential value was close to that of the mixture of pristine nanoparticles (SiO_2/ $CaCO_3$) and XRD exhibited peaks corresponding to $CaCO_3$ and a bump corresponding to SiO_2.

A noticeable influence of the EVA-matrix on the soot size was illustrated by the presence of same particle size in comparison with the matrix. One can note that the average carbon particles size in nanocomposite soot (54.9 nm) was quite similar to the initial value of 63.6 nm obtained for EVA. As Ounoughene et al. Ounoughene et al., [22] have shown the PDMS incineration promotes three kinds of particles size population (less than 20 nm, around 50 nm and up to 100 nm). In this study similar partitioning was obtained in PDMS soot. However, only intermediate and bigger particles were observed in PDMS nanocomposite soot. This phenomenon seems to be linked to the agglomeration/aggregation of the particles in the presence of nanoparticle mixture, according to DLS measurements.

The analysis of the results obtained shows that a priori the nanoparticles remain mainly in the

residues, even if the results seem to depend on the nature and the rate of nanoparticles as well as on the chemical composition of the polymer matrix used to formulate the nanocomposites.

Moreover, analyses of residues showed the presence of nanoparticles for both polymers and that their initial crystalline structure was maintained. Silica and calcium carbonate nanoparticles were found in soot for all matrices. Image analysis highlighted that the presence of nanoparticles in soot did not entail significant agglomeration/aggregation phenomena.

The discussion of the behaviour and fate of nanomaterials in waste has shown that EVA does not produced soot after incineration. But the presence of nanoparticles can generate residual ash. The different characterizations performed on PA-6/PP + ZnO nanocomposite show ZnO nanoparticles found in the residues is agglomerated/aggregated with composite particles with carbonaceous structures. (ref article). In addition, the presence of ZnO nanoparticles can also affect the recovery of ZnO-nanoparticles in residual ash, which needs to be taken into consideration when dealing with toxicity of waste. Thus, at lab-scale study, resembling waste incineration, simulation of a mixture of nanoparticles and matrixes in waste. For comparison, the by-products of the nanocomposites are also represented in the Table 5.

Table 5
Summary of location of by-products generated by the mixture of 3 polymers and 3 nanoparticles.

Nanocomposites Matrix	**Initial nanoparticles**	**Incineration by-products**	
		Soot	Residue
PA−6/PP + EVA	**ZnO +SiO_2 / $CaCO_3$**	Oxygen, Carbon	Carbon, Oxygen, Silicon, Calcium, Zinc

The presence of all nanoparticles in residue improve the understanding of nanocomposite degradation during incineration and the composition of the waste, including the presence of a mix of nanomaterials. Accumulation of nanowaste in residue raised the crucial point of the toxicological profile of this mixture, including uncertainties about the synergistic or antagonist effects of a mix of nanomaterials. Toxicological profile from the by-products emitted by mixture of SiO_2/$CaCO_3$ in nanocomposite-based EVA or PDMS.

The toxicity profiles of the EVA or PDMS polymer blends with a mixture of nanoparticles (SiO_2 + $CaCO_3$) were compared in the summarizing Table 6.

The main conclusion is that concerning the mixture of SiO_2/$CaCO_3$ nanoparticles, whatever the matrix considered (EVA or PDMS), the biological activities of the residues and the soot are always linked to those of the silica particles. We can attribute this effect to silica, knowing that $CaCO_3$ has been shown to have no toxicological signature.

The mixture of pristine particles SiO_2/$CaCO_3$ were not cytotoxic but induced a high pro-inflammatory response. Concerning the nanocomposite, the toxicity profile was mainly governed by the thermal degradation matrix pathway. The major impact is observed with pro-inflammatory responses whatever the matrix. About the soot, the nanoparticles released from PDMS nanocomposite, slightly increased the pro-inflammatory response compared to PDMS alone, although the morphology of the particles was similar. On the opposite, the mixture of nanoparticles impacts the nature of molecules released during the incineration of EVA nanocomposite leading to residue with a pro-inflammatory response increase. Indeed, the mixture of nanoparticles drives the composition of soot effluents and consequently the pro-inflammatory response decreases drastically vs pristine EVA. So, the compounds responsible of the pro-inflammatory response remain trapped in the residue when the nanoparticles mixture is used. The results of the LDH release assay, corresponding to cell membrane damage and thus the cytotoxicity induced, showed that at the highest dose in the PDMS with or without mixture of nanoparticles triggered a similar cytotoxicity either in residue or in soot. The nanoparticles mixture did not induce significant cytotoxicity. After 90 min or 24 h of cell-sample contact, mixture of SiO_2 / $CaCO_3$ nanoparticles did not exhibit a significant ROS production compared to that of the control (unexposed) cells.

Regarding the SiO_2/$CaCO_3$ nanoparticle mixture, whatever the matrix considered (EVA or PDMS), the biological activities of the residues and soot are always linked to those of the silica particles. We can attribute this effect to silica from nanoparticles incorporated in the matrix and, not given by the presence of $CaCO_3$ which have no toxicological signature. Furthermore, we note that the addition of $CaCO_3$ does not reduce the impact of silica (dilution) on toxicological responses.

4.2. Exploration of a potentially synergistic/ antagonist effect on biological outcomes by a mixture of nanoparticles (SiO_2/$CaCO_3$) in EVA-nanocomposite incinerated with a mixture of polymers (PA-6/PP) containing ZnO nanoparticles

As reported in Supplementary data (Figs. S7, S8 and S9), we also assessed the toxicity of the by-products obtained after the incineration of a complex mix consisting of 2 matrices (EVA and PA6/PP) and 3 nanoparticles (ZnO, SiO_2 and $CaCO_3$). Such mixture is more representative of real-life scenarios where nanowastes from different sources can be combined.

Table 6
Toxicological profile of the end-by products from EVA and PDMS samples, pristine or filled with a mixture of nanoparticles ($SiO_2/CaCO_3$), in comparison to that of pristine $SiO_2/CaCO_3$ mixture. *n.s: non significant; +: low; ++: moderate;+++: high.*

	Pristine	Polymers				Composites			
	$SiO_2/CaCO_3$	PDMS		EVA		PDMS + $SiO_2/CaCO_3$		EVA + $SiO_2/CaCO_3$	
		Residue	Soot	Residue	Soot	Residue	Soot	Residue	Soot
Cytotoxicity (LDH)	n.s.	++	+	No residue	n.s.	++	+	n.s.	+
Pro-inflammatory response (TNF-α)	+++	+++	++	No residue	+++	+++	+++	+++	+
Oxidative stress (ROS) 90 min and 24 h	n.s.	n.s.	n.s.	No residue	n.s.	n.s.	n.s.	n.s.	n.s.

Table 7
New insight on more realistic nanowaste stream toxicity provided by a complex mixture consisting of 2 matrices (EVA and PA6/PP) and 3 nanoparticles (ZnO, SiO_2 and $CaCO_3$). *n.s: non significant; +: low; ++: moderate;+++: high.*

	Pristine nanoparticles		Composites				Mixture of composites	
	$SiO_2/CaCO_3$	ZnO	PA-6/PP + ZnO		EVA + $SiO_2/CaCO_3$		PA-6/PP + ZnO and EVA + $SiO_2/CaCO_3$	
			Residue	Soot	Residue	Soot	Residue	Soot
Cytotoxicity (LDH)	*n.s*	+	*n.s*	*n.s*	*n.s*	++	*n.s*	+
Pro-inflammatory response (TNF-α)	++	+	++	*n.s*	+++	+	++	+
Oxidative stress (ROS) 90 min and 24 h	*n.s*	*n.s*	*n.s*	*n.s*	*n.s*	*n.s*	*n.s*	*n.s*

The Table 7 proposes a summary of potential toxicity regarding nanowaste stream provided by a mixture of nanocomposite. Low pro-inflammatory response was governed by the presence of pristine $SiO_2/CaCO_3$ mixture in soot whatever the matrices. Moderate pro-inflammatory response was obtained due to an antagonistic phenomenon caused by the presence of ZnO. In some cases, such as this one, mixing nanoparticles can have a positive impact on reducing the toxic potential of incineration residues, while polymer matrices generate no residues at all. Only the nature of the nanoparticles can generate toxicity. This study must be supplemented by other types of polymers that could generate residues during their own degradation.

5. Conclusion

The aim of this work was to study the physicochemical transformations and the hazard profile of nanowaste (residues and soot) resulting from the incineration process of nanocomposites formulated with mixtures of nanoparticles (SiO_2 and $CaCO_3$) that are widely used in the composition of electrical wires and cables. A wide range of instrumental techniques dedicated to the characterization of the incineration by-products was used to achieve this objective: SEM, BET, DLS, Zeta potential, XRD.

This work mainly showed that the mixture of silica and calcium carbonate nanoparticles always remained in the residue. *In vitro* toxicological profiles clearly demonstrated that only pro-inflammatory responses seemed to be affected by the presence of the nanoparticles. Moreover, this study showed that the silica nanoparticles have a major impact on toxicity whatever the partitioning in soot or residue, regardless the matrices. On the opposite, the addition of $CaCO_3$ did not provide the expected impact to reduce the nanowaste toxicity and did not seem really able to mitigate the SiO_2 toxicity.

As Schwab et al. underlined recently [37], a large variety of nanomaterials, and complex mixture nanowastes were not discussed in detail in literature and a global regulation on nanowaste is still pending. To conclude, the nanowaste residue tends to be agglomerated/aggregated and could be combined with other nanowastes in various processes. So, studies dedicated to the mixing of nanoparticles and nanocomposites in waste streams during incineration seem necessary. Moreover, the current data available, about existing nanomaterials on the EU market, shows the difficulty to give the quantitative data of nanomaterials in different waste stream. The lack of quantitative information about nanowaste creates some challenges. In this context, guidance on waste flow from nanocomposites incineration is an important step to facilitate practical actions in managing nanowaste.

In this context, the ECHA study alerts the society about the hazardous of nanocomposites end of life and answers the scientists about the solutions to be developed in order to reduce the environmental impact. Currently, the studies are focused on the incineration behaviour of only one nanocomposite without taking into account the potential synergetic or antagonistic impact of potential hazardous nanowastes on the toxicological profile.

Our first new insight of nanowaste stream investigated in this paper highlights the need to characterize the residual ash whatever the mixture of matrices and nanoparticles. Further studies on the simultaneous incineration of nanocomposites mixtures with combination of nanoparticles (toxic or non-toxic) would allow databases to be updated. The mechanisms induced by these mixtures are not currently investigated, but it would enable to predict the risks of the generated nanowastes.

CRediT authorship contribution statement

Claire LONGUET: Methodology, Formal analysis, Writing – original draft, review & editing, Conceptualization, Supervision. **Carine Chivas-Joly:** Methodology, Formal analysis, Investigation, Conceptualization, review & editing, Writing. **Nora Lambert:** Investigation. **Valérie Forest:** Methodology, Formal analysis, Conceptualization, review & editing, Writing. **Lara Leclerc:** Methodology, Formal analysis, Investigation, Writing. **Gwendoline Sarry:** Investigation.**Jérémie Pourchez:** Methodology, Formal analysis, Conceptualization, review & editing, Writing. **José-Marie Lopez-Cuesta:** Review & editing, Writing.

Declaration of Competing Interest

The authors declare the following financial interests/personal relationships which may be considered as potential competing interests: Claire LONGUET reports financial support was provided by The French Agency for Ecological Transition. Claire LONGUET reports a relationship with The French Agency for Ecological Transition that includes: funding grants. If there are other authors, they declare that they have no known competing financial interests or personal relationships that could have appeared to influence the work reported in this paper.

Acknowledgements

The authors are grateful to the French Environment and Energy

Management Agency (ADEME) under grant no 1906C0012 for the financial support provided to the NANODETOX project and especially to Isabelle DEPORTES for her support during this project. We want to thankful Dr. Belkacem OTAZAGHINE for its kindly support in Py-GC/MS measurements and analyses, Pr. Gwenn LE SAOULT for its kindly support in XRD and Benjamin GALLARD for the formulations performing. We acknowledge Dr. Simon DELCOUR and Frederic DE LAGOS for nanocomposites incineration at LNE.

Appendix A. Supporting information

Supplementary data associated with this article can be found in the online version at doi:10.1016/j.nxnano.2024.100113.

References

[1] Thomas, S., Vahabi, H., Somasekharan, L., 2024. Flame Retardant Nanocomposites - Emergent Nanoparticles and Their Applications.
[2] Global plastic production, 2022. Statista. URL ⟨https://www.statista.com/statistics/282732/global-production-of-plastics-since-1950/⟩ (accessed 8.23.24).
[3] J. Troitzsch, E. Antonatus, Electrical engineering and cables, in: Plastics Flammability Handbook, Carl Hanser Verlag GmbH & Co. KG, 2021, pp. 647–728, https://doi.org/10.3139/9781569907634.012.
[4] J. Cogen, T. Lin, P. Whaley, Material Design for Fire Safety in Wire and Cable Applications, CRC Press, 2009, pp. 783–808, https://doi.org/10.1201/9781420084009-c26.
[5] C. Lagreve, L. Ferry, J.-M. Lopez-Cuesta, Flame retardant polymer materials design for wire and cable applications, in: Flame Retardant Polymeric Materials, CRC Press, 2019.
[6] D. Singh, A. Marrocco, W. Wohlleben, H.-R. Park, A.R. Diwadkar, B.E. Himes, Q. Lu, D.C. Christiani, P. Demokritou, Release of particulate matter from nano-enabled building materials (NEBMs) across their lifecycle: potential occupational health and safety implications, J. Hazard. Mater. 422 (2022) 126771, https://doi.org/10.1016/j.jhazmat.2021.126771.
[7] D. Singh, W. Wohlleben, R. De La Torre Roche, J.C. White, P. Demokritou, Thermal decomposition/incineration of nano-enabled coatings and effects of nanofiller/matrix properties and operational conditions on byproduct release dynamics: potential environmental health implications, NanoImpact 13 (2019) 44–55, https://doi.org/10.1016/j.impact.2018.12.003.
[8] G.A. Sotiriou, D. Singh, F. Zhang, M.-C.G. Chalbot, E. Spielman-Sun, L. Hoering, I. G. Kavouras, G.V. Lowry, W. Wohlleben, P. Demokritou, Thermal decomposition of nano-enabled thermoplastics: possible environmental health and safety implications, J. Hazard. Mater. 305 (2016) 87–95, https://doi.org/10.1016/j.jhazmat.2015.11.001.
[9] European Chemicals Agency (EU body or agency), Risk & Policy Analysts Ltd, RPA Europe Srl, Z. Manžuch, R. Akelytė, R. Perez García, G. Kriščiūnaitė, M. Camboni, D. Carlander, Study on the Product Lifecycles, Waste Recycling and the Circular Economy for Nanomaterials: November 2021, Publications Office of the European Union, LU, 2021.
[10] OECD, 2018. Publications in the Series on the Safety of Manufactured Nanomaterials - OECD URL ⟨https://www.oecd.org/env/ehs/nanosafety/publications-series-safety-manufactured-nanomaterials.htm⟩ (accessed 9.20.23).
[11] Baumann, W., Teuscher, N., Hauser, M., Gehrmann, J., Paur, H.-R., Stapf, D., 2017. Behaviour of Engineered Nanoparticles in A Lab-scale Flame and Combustion Chamber. Energy Procedia, INFUB - 11th European Conference on Industrial Furnaces and Boilers, INFUB-11 120, 705–712. https://doi.org/10.1016/j.egypro.2017.07.194.
[12] C. Chivas-Joly, C. Longuet, J. Pourchez, L. Leclerc, G. Sarry, J.-M. Lopez-Cuesta, Physical, morphological and chemical modification of Al-based nanofillers in by-products of incinerated nanocomposites and related biological outcome, J. Hazard. Mater. 365 (2019) 405–412, https://doi.org/10.1016/j.jhazmat.2018.10.029.
[13] T. Fujimori, A. Toda, K. Mukai, M. Takaoka, Incineration of carbon nanomaterials with sodium chloride as a potential source of PCDD/Fs and PCBs, J. Hazard. Mater. 382 (2020) 121030, https://doi.org/10.1016/j.jhazmat.2019.121030.
[14] A.L. Holder, E.P. Vejerano, X. Zhou, L.C. Marr, Nanomaterial disposal by incineration, Environ. Sci. Process. Impacts 15 (2013) 1652–1664, https://doi.org/10.1039/C3EM00224A.
[15] F. Part, N. Berge, P. Baran, A. Stringfellow, W. Sun, S. Bartelt-Hunt, D. Mitrano, L. Li, P. Hennebert, P. Quicker, S.C. Bolyard, M. Huber-Humer, A review of the fate of engineered nanomaterials in municipal solid waste streams, Waste Manag. 75 (2018) 427–449, https://doi.org/10.1016/j.wasman.2018.02.012.
[16] J. Pourchez, C. Chivas-Joly, C. Longuet, L. Leclerc, G. Sarry, J.-M. Lopez-Cuesta, End-of-life incineration of nanocomposites: new insights into nanofiller partitioning into by-products and biological outcomes of airborne emission and residual ash, Environ. Sci. Nano 5 (2018) 1951–1964, https://doi.org/10.1039/C8EN00420J.
[17] D. Singh, G.A. Sotiriou, F. Zhang, J. Mead, D. Bello, W. Wohlleben, P. Demokritou, End-of-life thermal decomposition of nano-enabled polymers: effect of nanofiller loading and polymer matrix on by-products, Environ. Sci. Nano 3 (2016) 1293–1305, https://doi.org/10.1039/C6EN00252H.
[18] OECD, 2016. Nanomaterials in Waste Streams: Current Knowledge on Risks and Impacts | en OECD, URL ⟨https://www.oecd.org/chemicalsafety/nanomaterials-in-waste-streams-9789264249752-en.htm⟩ (accessed 9.20.23).
[19] E.P. Vejerano, E.C. Leon, A.L. Holder, L.C. Marr, Characterization of particle emissions and fate of nanomaterials during incineration, Environ. Sci. Nano 1 (2014) 133–143, https://doi.org/10.1039/C3EN00080J.
[20] G.A. Sotiriou, D. Singh, F. Zhang, W. Wohlleben, M.-C.G. Chalbot, I.G. Kavouras, P. Demokritou, An integrated methodology for the assessment of environmental health implications during thermal decomposition of nano-enabled products, Environ. Sci. Nano 2 (2015) 262–272, https://doi.org/10.1039/C4EN00210E.
[21] G. Ounoughene, Etude des émissions liées à la décomposition thermique de nanocomposites: application à l'incinération (These de doctorat), Ecole des Mines, Nantes, 2015.
[22] G. Ounoughene, C. Chivas-Joly, C. Longuet, O. Le Bihan, J.-M. Lopez-Cuesta, L. Le Coq, Evaluation of nanosilica emission in polydimethylsiloxane composite during incineration, J. Hazard. Mater. 371 (2019) 415–422, https://doi.org/10.1016/j.jhazmat.2019.03.026.
[23] G. Ounoughene, O. Le Bihan, C. Chivas-Joly, C. Motzkus, C. Longuet, B. Debray, A. Joubert, L. Le Coq, J.-M. Lopez-Cuesta, Behavior and fate of halloysite nanotubes (HNTs) when incinerating PA6/HNTs nanocomposite, Environ. Sci. Technol. 49 (2015) 5450–5457, https://doi.org/10.1021/es505674j.
[24] C. Watson-Wright, D. Singh, P. Demokritou, Toxicological implications of released particulate matter during thermal decomposition of nano-enabled thermoplastics, NanoImpact 5 (2017) 29–40, https://doi.org/10.1016/j.impact.2016.12.003.
[25] C. Chivas-Joly, C. Longuet, L. Leclerc, G. Sarry, V. Forest, J.-M. Lopez-Cuesta, J. Pourchez, Physicochemical characterization and toxicity of nanowaste after incineration process of PA-6/PP/ZnO or TiO_2 nanocomposites, Environ. Sci. Nano 9 (2022) 4570–4584, https://doi.org/10.1039/D2EN00630H.
[26] B.S. Babu, K. Kumar, Nanomaterials and Nanocomposites: Characterization, Processing, and Applications (Eds.), CRC Press, Boca Raton, 2021, https://doi.org/10.1201/9781003160946.
[27] ISO/TC 229 - Nanotechnologies, 2021. ISO. URL ⟨https://www.iso.org/fr/committee/381983.html⟩ (accessed 9.20.23).
[28] ISO/TR 13014:2012, 2012. ISO. URL ⟨https://www.iso.org/fr/standard/52334.html⟩ (accessed 9.20.23).
[29] Foucher, J., Labrosse, A., Dervillé, A., Zimmermann, Y., Bernard, G., Martinez, S., Grönqvist, H., Baderot, J., Pinzan, F., 2017. The Coming of Age of the First Hybrid Metrology Software Platform Dedicated to Nanotechnologies (Conference Presentation) [WWW Document]. URL ⟨https://www.spiedigitallibrary.org/conference-proceedings-of-spie/10145/1014507/The-coming-of-age-of-the-first-hybrid-metrology-software/10.1117/12.2258093.short?SSO=1⟩ (accessed 9.20.23).
[30] N. Bouzakher-Ghomrasni, O. Taché, J. Leroy, N. Feltin, F. Testard, C. Chivas-Joly, Dimensional measurement of TiO_2 (Nano) particles by SAXS and SEM in powder form, Talanta 234 (2021) 122619, https://doi.org/10.1016/j.talanta.2021.122619.
[31] W. Wohlleben, J. Mielke, A. Bianchin, A. Ghanem, H. Freiberger, H. Rauscher, M. Gemeinert, V.-D. Hodoroaba, Reliable nanomaterial classification of powders using the volume-specific surface area method, J. Nanopart. Res 19 (2017) 61, https://doi.org/10.1007/s11051-017-3741-x.
[32] N.B. Ghomrasni, C. Chivas-Joly, L. Devoille, J.-F. Hochepied, N. Feltin, Challenges in sample preparation for measuring nanoparticles size by scanning electron microscopy from suspensions, powder form and complex media, Powder Technol. 359 (2020) 226–237, https://doi.org/10.1016/j.powtec.2019.10.022.
[33] L. Leclerc, D. Boudard, J. Pourchez, V. Forest, O. Sabido, V. Bin, S. Palle, P. Grosseau, D. Bernache, M. Cottier, Quantification of microsized fluorescent particles phagocytosis to a better knowledge of toxicity mechanisms, Inhal. Toxicol. 22 (2010) 1091–1100, https://doi.org/10.3109/08958378.2010.522781.
[34] L. Leclerc, W. Rima, D. Boudard, J. Pourchez, V. Forest, V. Bin, P. Mowat, P. Perriat, O. Tillement, P. Grosseau, D. Bernache-Assollant, M. Cottier, Size of submicrometric and nanometric particles affect cellular uptake and biological activity of macrophages in vitro, Inhal. Toxicol. 24 (2012) 580–588, https://doi.org/10.3109/08958378.2012.699984.
[35] K.S.P. Karunadasa, C.H. Manoratne, H.M.T.G.A. Pitawala, R.M.G. Rajapakse, Thermal decomposition of calcium carbonate (calcite polymorph) as examined by in-situ high-temperature X-ray powder diffraction, J. Phys. Chem. Solids 134 (2019) 21–28, https://doi.org/10.1016/j.jpcs.2019.05.023.
[36] E. Delebecq, S. Hamdani-Devarennes, J. Raeke, J.-M. Lopez Cuesta, F. Ganachaud, High residue contents indebted by platinum and silica synergistic action during the pyrolysis of silicone formulations, ACS Appl. Mater. Interfaces 3 (2011) 869–880, https://doi.org/10.1021/am101216y.
[37] F. Schwab, B. Rothen-Rutishauser, A. Scherz, T. Meyer, B.B. Karakoçak, A. Petri-Fink, The need for awareness and action in managing nanowaste, Nat. Nanotechnol. 18 (2023) 317–321, https://doi.org/10.1038/s41565-023-01331-4.